数理解析研究所講究録 第2109巻 2019年 70-76

Transverse Instability of Surface Solitary Waves and Breaking

Takeshi KATAOKA

Graduate School of Engineering, Kobe University

Abstract

The linear stability of finite-amplitude surface solitary waves with respect to transverse perturbations (three-dimensional perturbations) is studied on the basis of the Euler set of equations. First, the linear stability to long-wavelength transverse perturbations is examined, and it is found that there exist transversely unstable surface solitary waves for the amplitude-to-depth ratio of over 0.713 (Kataoka & Tsutahara 2004). This critical ratio is well below that (=0.781) for the longitudinal instability obtained by Tanaka (1986). Next, the same transverse instability is examined numerically and we find that results are consistent with the above analytical results in that the growth rates and the eigenfunctions of growing disturbance modes agree well with those obtained by the theory (Kataoka 2010). Finally, time evolution of transversely distorted solitary wave is simulated numerically in order to give clear intuitive picture of unstable wave motion. In this report we only treat the final topic on numerical simulation of a distorted solitary wave since the first two topics were already published.

1. INTRODUCTION

We carry out numerical simulation of a surface solitary wave in order to demonstrate the existence of transversely unstable surface solitary waves, which was analytically proved by Kataoka & Tsutahara (2004). Transverse stability means a stability to disturbances that depend not only on the main wave travelling direction, but also on its transverse direction. In contrast, longitudinal stability is a stability to disturbances that depend only on the main wave travelling direction. Choosing the solitary wave solution whose crest is distorted periodically in the transverse direction as the initial condition, we simulate its time evolution numerically on the basis of the three-dimensional Euler equations. It is then confirmed that there really exist transversely unstable solitary waves which are longitudinally stable.

As for the linear stability analysis, Tanaka (1986) first examined the longitudinal stability on the basis of the Euler equations, and discovered that the longitudinal instability occurs for the surface solitary waves whose maximum surface displacement is greater than 0.781 times the undisturbed depth of the fluid. Tanaka et al. (1987) also conducted numerical simulation to study the time development of a surface solitary wave disturbed by a longitudinal disturbance, and found that the growth rate of sufficiently small disturbance agrees well with that of the linear stability analysis. The more precise linear stability analysis was carried out later by Longuet-Higgins & Tanaka (1997).

The transverse stability of surface solitary waves was examined by Kataoka & Tsutahara (2004). The criterion of transverse instability is derived analytically, and it is found that the surface solitary waves are transversely unstable if the maximum surface displacement is greater than 0.713 times the undisturbed depth of the fluid. This critical amplitude is well below that (=0.781) for the longitudinal instability. This transverse instability is, however, proved only for the case where the transverse wavelength of a disturbance is very long. It is, therefore, desired that this transverse instability is confirmed by numerical simulation when a disturbance has some finite transverse wavelength. It would be also useful to show how the unstable solitary wave evolves as time elapses.

In the present report, therefore, we will show some numerical results on time evolution of a transversely distorted surface solitary wave, and demonstrate that there really exist transversely unstable surface solitary wave which is 2D stable. It is also shown that there is a high transverse wavenumber cutoff for this transverse instability.

2. PROBLEM AND BASIC EQUATIONS

Consider the three-dimensional irrotational flow of an incompressible ideal fluid of undisturbed depth D with free surface under uniform acceleration due to gravity g (Fig. 1). The effect of surface tension is neglected. In what follows, all variables are non-dimensionalized using g and D. Introducing the Cartesian coordinates x, y, z with the z-axis pointed vertically upward and its origin placed on the undisturbed free surface, we obtain the following set of non-dimensional governing equations for the flow:

$$\nabla^2\phi = 0 \quad \text{for} \quad -1 < z < \eta, \tag{1}$$

$$\frac{\partial\phi}{\partial z} = 0 \quad \text{at} \quad z = -1, \tag{2}$$

$$\frac{\partial\eta}{\partial t} + \frac{\partial\phi}{\partial x}\frac{\partial\eta}{\partial x} + \frac{\partial\phi}{\partial y}\frac{\partial\eta}{\partial y} = \frac{\partial\phi}{\partial z} \quad \text{at} \quad z = \eta, \tag{3}$$

$$\frac{\partial\phi}{\partial t} + \eta + \frac{1}{2}\left[\left(\frac{\partial\phi}{\partial x}\right)^2 + \left(\frac{\partial\phi}{\partial y}\right)^2 + \left(\frac{\partial\phi}{\partial z}\right)^2\right] = 0 \quad \text{at} \quad z = \eta, \tag{4}$$

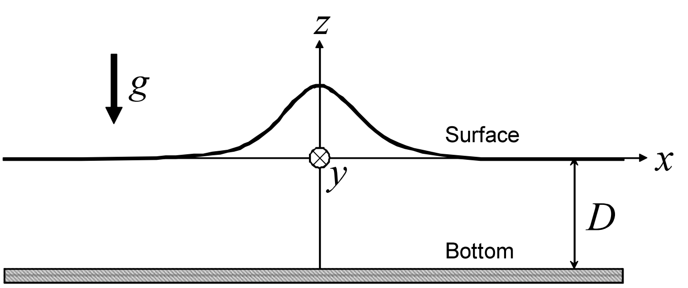

Fig. 1 Geometry.

where

$$\nabla^2 = \frac{\partial^2}{\partial x^2} + \frac{\partial^2}{\partial y^2} + \frac{\partial^2}{\partial z^2}, \tag{5}$$

and $\phi(x,y,z,t)$ is the velocity potential, $\eta(x,y,t)$ is the vertical displacement of the free surface, and t is the time.

Let us first consider a steady solution of (1)-(4) in the following form:

$$\begin{cases} \phi = -vx + \Phi_s(x,z), \\ \eta = \eta_s(x), \end{cases} \tag{6}$$

where $\partial\Phi_s/\partial x$, $\partial\Phi_s/\partial z$, and η_s approach zero as $x \to \pm\infty$, and v is a positive real parameter. This solution represents a steady propagation of localized wave against a uniform stream of constant velocity $-v$ in the x-direction. We call this solution a solitary wave solution. The existence of such a solitary wave solution has already been confirmed numerically. The solution is characterized by a single parameter v, but for a clear intuitive picture of wave form, we here use another parameter, the dimensionless maximum surface displacement

$$\eta_{\max} \equiv \max|\eta_s|. \tag{7}$$

The solitary wave solution (6) is known to exist for $0 < \eta_{\max} < 0.833$, and stable with respect to two-dimensional disturbances (which depend on x and z) for $0 < \eta_{\max} < 0.781$ (Tanaka 1986). This solitary wave solution can be obtained numerically by the method described in Tanaka (1986).

Here we will numerically simulate time evolution of the above solitary wave when its crest is distorted periodically with respect to y. The corresponding initial condition is specifically given by

$$\begin{cases} \phi = -vx + \Phi_s\left(x + P_{\max}\cos\dfrac{\pi y}{Y_{\max}}, z\right), \\ \eta = \eta_s\left(x + P_{\max}\cos\dfrac{\pi y}{Y_{\max}}\right), \end{cases} \text{at } t = 0, \tag{8}$$

where $P_{\max}$ and $Y_{\max}$ are given constants representing amplitude and transverse wavelength of a disturbance, respectively. From symmetry, we can impose an impermeable condition at $y = 0$ and $Y_{\max}$, i.e.

$$\frac{\partial\phi}{\partial y} = 0 \quad \text{at} \quad y = 0, Y_{\max}. \tag{9}$$

Thus, the problem is reduced to an initial-boundary value problem of (1)-(4) under the initial condition (8) and the boundary condition (9) at $y = 0$ and $Y_{\max}$. The parameters are $\eta_{\max}$, $P_{\max}$, and $Y_{\max}$. The numerical method to solve this problem is described in Section 3.

3. NUMERICAL METHOD

The boundary conditions (3) and (4) at the surface $z=\eta$ can be reformulated as follows:

$$\frac{\partial \eta}{\partial t} - v\eta_x = \tilde{\phi}_n \sqrt{1+\eta_x^2+\eta_y^2} \quad \text{at} \quad z=\eta, \tag{10}$$

$$\frac{\partial \tilde{\phi}}{\partial t} - v\tilde{\phi}_x + \eta - \frac{\tilde{\phi}_n^2}{2} - \frac{\tilde{\phi}_x\eta_x + \tilde{\phi}_y\eta_y}{\sqrt{1+\eta_x^2+\eta_y^2}}\tilde{\phi}_n + \frac{\left(\tilde{\phi}_x\eta_y - \tilde{\phi}_y\eta_x\right)^2 + \tilde{\phi}_x^2 + \tilde{\phi}_y^2}{2\left(1+\eta_x^2+\eta_y^2\right)} = 0 \quad \text{at} \quad z=\eta, \tag{11}$$

where $\tilde{\phi}(x,y,t)$ is the velocity potential relative to the uniform stream evaluated at $z=\eta$, or $\tilde{\phi}(x,y,t)=\phi(x,y,\eta,t)+vx$, and the subscripts x and y denote the partial differentiation with respect to x and y, respectively (e.g. $\tilde{\phi}_x \equiv \partial\tilde{\phi}/\partial x = \partial\phi/\partial x + v + (\partial\phi/\partial z)(\partial\eta/\partial x)$). $\tilde{\phi}_n$ is the derivative upward normal to the surface of $\phi + vx$ evaluated at $z=\eta$.

Using the Green's formulation, we can obtain ϕ_n at the free surface in terms of $\tilde{\phi}$ as the solution of the following integral equation:

$$\iint_{\text{all } S}\left(\tilde{\phi}'\frac{\partial G}{\partial n'} - \tilde{\phi}_n' G\right)\mathrm{d}S' = -2\pi\tilde{\phi}, \tag{12}$$

where the functions with a prime denote those at (x',y'). S represents the free surface and dS' the corresponding infinitesimal element which includes (x',y'). The function G is Green's function of the three-dimensional Laplace equation (1) that satisfies $\nabla^2 G = -4\pi\delta(x-x',y-y',z-z')$ and $\partial G/\partial z' = 0$ at $z'=-1$, where δ is the Dirac delta function. It is specifically given by

$$G(x,y,z,x',y',z') = \frac{1}{r} + \frac{1}{\bar{r}}, \tag{13}$$

where

$$r = \sqrt{(x-x')^2+(y-y')^2+(z-z')^2}, \quad \bar{r} = \sqrt{(x-x')^2+(y-y')^2+(z+z'+2)^2}. \tag{14}$$

The set of equations for $\tilde{\phi}$ and η is given by (10)-(12).

The derivatives of $\tilde{\phi}$ and η with respect to x and y in (10)-(12) are evaluated by the eighth-order finite-difference method. $\tilde{\phi}_n$ is obtained from the boundary integral equation (12) in which the integral is evaluated by the boundary element method (see Grilli et al. (2001) for details).

The computational domain is $-30 < x < 20$, $0 < y < Y_{\max}$. The number of grids is 200 (in the x direction)$\times$32 (in the y direction). The grid points in the x direction are concentrated toward $x=0$ to capture the motion of the solitary wave with higher accuracy. In the y direction, these are equally distributed. We apply a uniform-stream condition at the upstream boundary $x=20$, and the radiation condition (Pearson 1974) at the downstream boundary $x=-30$, which is expressed as

$$\frac{\partial \tilde{\phi}}{\partial t} - v\frac{\partial \tilde{\phi}}{\partial x} = 0, \quad \frac{\partial \eta}{\partial t} - v\frac{\partial \eta}{\partial x} = 0. \tag{15}$$

Small disturbances are radiated downstream from the solitary wave due to its distortion and arrive at the downstream boundary. So we need to evaluate the effect of this artificial open boundary. Indeed we have tested several cases where this open boundary is located much farther downstream and no detectable differences were found over the region $-20 < x < 20$.

4. NUMERICAL RESULTS

The present problem (1)-(4), (8), and (9) is characterized by three parameters: wave amplitude of the solitary wave $\eta_{\max}$, amplitude of a disturbance $P_{\max}$, and half wavelength of a disturbance in the y direction $Y_{\max}$ (Fig. 2). In order to demonstrate the existence of transversely unstable solitary waves, which was proved analytically when disturbances are infinitesimal (Kataoka & Tsutahara 2004), we here put the amplitude of the disturbance at some small values. We conducted calculation of $P_{\max} = 0.01$, 0.02, and 0.03, and the qualitative results of wave behavior are independent of $P_{\max}$. Here only the results for $P_{\max} = 0.03$ are presented.

Figure 3 shows time evolution of surface profiles at a particular cross section $y = 0$ when $\eta_{\max} = 0.76$ for three different values of $Y_{\max} = 10$, 20 and 30. For all cases, surface of a distorted solitary wave is subject to an oscillatory motion with respect to both x and z-axes. That is, the crest point of a distorted solitary wave traces an ellipse in the clockwise sense. After one cycle of this elliptic motion, in the next cycle, the crest point again traces an ellipse, but with some difference in its radius. Each figure shows the surface profile near the crest of the solitary wave on the cross section $y = 0$. The dashed line is the initial profile while the solid (red and blue) lines are those in the first (red) and second (blue) cycles, respectively. It is obvious from Fig.3 (a) that the maximum wave height in the second cycle is smaller than that in the first cycle. Figure 3 (b) shows, however, that the maximum wave height is almost unchanged in the first and second cycles, and figure 3 (c) clearly indicates that the maximum height is amplified in the second cycle. Thus, the solitary wave for $\eta_{\max} = 0.76$ is unstable to transverse perturbations of long half wavelength $Y_{\max} > 20$.

For the other values of $\eta_{\max}$, we find that the solitary wave is neutrally stable at around $Y_{\max} = 30$ for $\eta_{\max} = 0.74$ and at $Y_{\max} = 15$ for $\eta_{\max} = 0.78$ (figures are not shown). Let us now evaluate the transverse stability of the solitary wave by using the maximum-height difference at two extreme times of the same cycle. Specifically, if the ratio of the difference in the second cycle to that

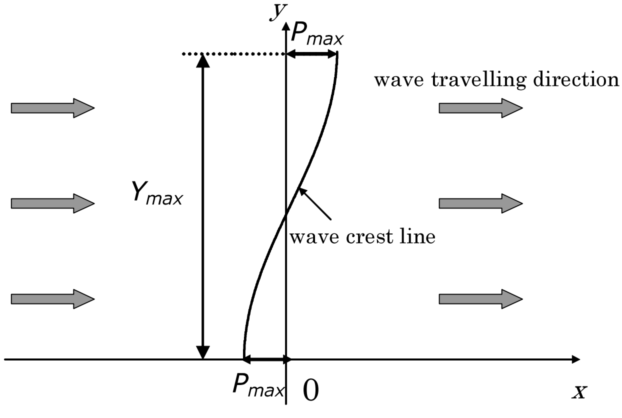

Fig. 2 Initial condition.

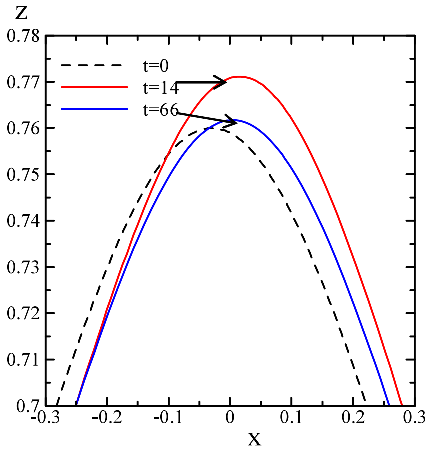

(a) $Y_{\max} = 10$

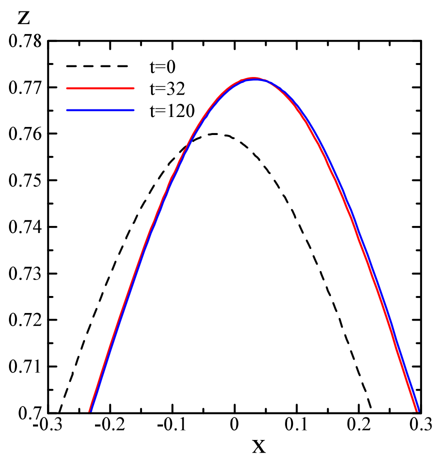

(b) $Y_{\max} = 20$

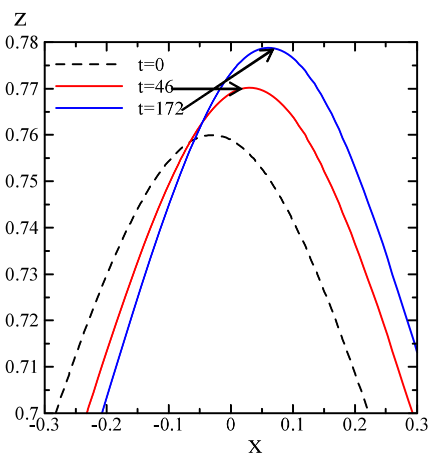

(c) $Y_{\max} = 30$

Fig. 3 Time development of a disturbed solitary wave for $\eta_{\max} = 0.76$ and $P_{\max} = 0.03$: (a) $Y_{\max} = 10$; (b) $Y_{\max} = 20$; (c) $Y_{\max} = 30$.

Table 1 Stability of solitary waves ($\eta_{\max} = 0.74$, 0.76, 0.78) to perturbations of transverse half wavelength $Y_{\max} = 10$, 20, 30, and 40.

$\eta_{\max} \setminus Y_{\max}$	10	20	30	40
0.74	stable	stable	neutral	unstable
0.76	stable	neutral	unstable	unstable
0.78	stable	unstable	unstable	unstable

in the first cycle is between 0.95 and 1.05, the solitary wave is defined to be neutrally stable. If it is larger than 1.05, the wave is defined as unstable and if smaller than 0.95, stable. The stability results based on this rule are arranged in Table 1. We can clearly see that there is a general tendency that the solitary wave is more unstable as $\eta_{\max}$ and $Y_{\max}$ become larger.

5. CONCLUDING REMARKS

Time evolution of transversely distorted surface solitary wave is numerically simulated on the basis of the three-dimensional Euler equations. It is demonstrated that there exist transversely unstable surface solitary waves that are longitudinally stable for $0.74 \le \eta_{\max} \le 0.78$. Specifically, it is confirmed that the initial distortion of the crest in the transverse direction increases as time elapses for $Y_{\max} > 30$, $Y_{\max} > 20$, and $Y_{\max} > 15$ when $\eta_{\max} = 0.74$, 0.76, and 0.78, respectively (results are shown here only for $\eta_{\max} = 0.76$). These results indicate that there is a short-wavelength cutoff to the transverse instability.

REFERENCES

Grilli, S.T., Guyenne, P., and Dias, F., "A fully non-linear model for three-dimensional overturning waves over an arbitrary bottom", *Intl J. Numer. Meth. Fluids* **35** (2001), pp.829-867.

Kataoka, T., "Transverse instability of surface solitary waves. Part 2. Numerical linear stability analysis", *J. Fluid Mech.* **657** (2010), pp.126-170.

Kataoka, T. and Tsutahara, M., "Transverse instability of surface solitary waves", *J. Fluid Mech.* **512** (2004), pp.211-221.

Longuet-Higgins, M. and Tanaka, M., "On the crest instabilities of steep surface waves", *J. Fluid Mech.* **336** (1997), pp.51-68.

Pearson, R.A., "Consistent boundary conditions for numerical models of systems that admit dispersive waves", *J. Atmos. Sci.* **31** (1974) p.1481.

Tanaka, M., "The stability of solitary waves", *Phys. Fluids* **29** (1986), pp.650-655.

Tanaka, M., Dold, J.W., Lewy, M., and Peregrine, D. H., "Instability and breaking of a solitary wave", *J. Fluid Mech.* **185** (1987), pp.235-248.